

# Compact Lossy Inductance Simulators With Electronic Control

M. Srivastava<sup>\*(C.A.)</sup> and K. Bhardwaj<sup>\*\*</sup>

**Abstract:** In this paper two R-L network simulator configurations employing a single VDDIBA, one resistance and one grounded capacitance are presented. The first configuration is a grounded series resistor-inductor (R-L) network simulator and the second configuration is intended for grounded parallel resistor-inductor (R-L) circuit simulation. Both the proposed circuits enjoy several beneficial features such as: 1) compact structure employing only one VDDIBA and two passive elements, 2) electronic tuning of inductive part of realized series/parallel R-L impedances, 3) independent control of inductive and resistive parts of realized parallel R-L impedance, 4) no requirement of any component matching, and 5) un-deviated performance in non-ideal environment. By choosing appropriate values of active/passive elements, a series R-L circuit for simulating resistance of 7.742 k $\Omega$  and inductance of value 7.742 mH has been developed. Similarly a parallel R-L simulation circuit to simulate a resistance of value 1 k $\Omega$  and inductance of value 77.4  $\mu$ H is implemented. To study the influence of parasitics on developed lossy inductances, the behavior of these configurations has been studied keeping terminal parasitics of VDDIBAs under consideration. To check the performance and usefulness of the proposed configurations some second-order filtering circuits have been designed. To confirm the theoretical analysis, PSPICE Simulation results have been included.

**Keywords:** Active RL Networks, Compact Circuit, Electronic Control, VDDIBA.

## 1 Introduction

An inductor is a very useful passive element which finds very frequent applications in circuits and electrical engineering. The working of conventional spiral inductors is not matched with the ideal behavior. The conventional spiral inductors also suffer from large weight and size, generation of undesired harmonics, electromagnetic radiations and strong parasitic effects. Therefore, in the last two decades, interest has been comprehensively directed towards the realization of synthetic inductors employing different active elements for simulating the behavior of passive conventional

inductors. Several grounded inductance realizations employing different active components have been described in open literature [1-8]. In addition to the simulation of lossless inductors, the simulation of lossy inductors is also found very useful. The grounded lossy inductance simulators have a wide range of applications covering series/parallel resonance circuits, filters and sinusoidal oscillators. Several grounded R-L (series/parallel) network simulation circuits employing numerous active elements such as OP-AMPs, current conveyors, current feedback amplifiers, Four terminal floating nullers, operational trans-resistance amplifiers, differential voltage current conveyor, current-feedback operational-amplifiers, dual X-current conveyors and voltage differential current conveyors have been introduced in literature [9-30]. On careful investigation of previously reported series/parallel R-L simulation circuits, it is observed that all these reported circuits have one or more of below given disadvantageous features:

- (i) Employment of excessive number of active building blocks (ABBs) (more than one);

Iranian Journal of Electrical and Electronic Engineering, 2019.

Paper first received 07 May 2018 and accepted 18 February 2019.

\* The author is with the NIT Jamshedpur, Jamshedpur (Jharkhand), India-831014.

E-mail: [mavank2780@gmail.com](mailto:mavank2780@gmail.com).

\*\* The author is with the KIET Group of Institutions, Ghaziabad (U. P.), India-201017.

E-mail: [kapilec143@gmail.com](mailto:kapilec143@gmail.com).

Corresponding Author: M. Srivastava.

- (ii) Employment of excessive number of passive components (more than two);
- (iii) Employment of floating capacitance(s);
- (iv) Lack of electronic control of realized equivalent resistances and inductances;
- (v) Non-availability of independent tuning of realized equivalent resistances and inductances and;
- (vi) Requirement(s) for matched active/passive components.

Therefore, the main aim of this article is to present new grounded lossy inductor simulators (series R-L, parallel R-L) with following useful features:

- (1) Employment of single active Element (VDDIBA);
- (2) Use of Two Passive Elements;
- (3) Use of single Grounded Capacitance;
- (4) Availability of Electronic Tuning of Realized Equivalent Inductance;
- (5) Availability of Non-Interactive Tuning Of Realized Inductance;
- (6) No Requirement of matched passive or active elements;
- (7) Excellent working under non-ideal constraints with no deviation;
- (8) Low Parasitic Effects.

The comparison of proposed grounded series R-L network simulator shown in Fig. 2 with previously proposed series R-L simulators has been given in Table 1. Similarly proposed grounded parallel R-L simulator (shown in Fig. 3) has been compared with previously reported parallel R-L simulators in Table 2.

## 2 Voltage Differencing Differential Input Buffered Amplifier (VDDIBA)

VDDIBA is a popular circuit idea proposed in [33]. It is a very useful ABB with electronic controllability feature. The symbolic block representation of VDDIBA is given in Fig. 1. VDDIBA has five input/output ports namely  $V_-$ ,  $V_+$ ,  $W$ ,  $V$ , and  $Z$ . The voltage difference of terminals  $V_+$  and  $V_-$  is transferred to  $Z$  terminal in the form of current. The voltage difference between the  $V$  and  $Z$  terminals is transferred at terminal  $W$  through a differential buffer of unity gain. The voltage-current relationships between different ports of VDDIBA have been given by Eqs. (1)-(3) in static (steady-state situation). The implementation of VDDIBA circuit concept using operational transconductance amplifiers (OTAs) and current feedback operational amplifier (CFOA) is demonstrated in Fig. 2. The CMOS realization of OTAs used in Fig. 2 has been shown in Fig. 3.

$$I_Z = \beta_Z g_m (V_{V_+} - V_{V_-}) \quad (1)$$

$$V_W = V_Z - V_V \quad (2)$$

$$I_{V_+} = I_{V_-} = I_V = 0 \quad (3)$$

The use of VDDIBA in various analog signal processing circuits has been discussed in [34-37]. Grounded lossless inductor simulator employing positive type VDDIBA has been discussed in [34] which employ two

**Table 1** Comparison of proposed series R-L simulator with previously reported series R-L simulation circuits.

Ref.	Fig. No.	No. of Active Element	No. of Resistors	No. of Capacitors	Electronic Control of $L_{eq}$ and $R_{eq}$	Non-Interactive Control of $L_{eq}$	Need for Element Matching
[10]	Fig. 2(a)	1	1(F)+1(G)	1(F)	No	No	No
[11]	Fig. 1	1	1(F)+1(G)	1(F)	No	No	No
	Fig. 2	2	1(F)+1(G)	1(F)	No	Yes	No
	Fig. 2	2	2(F)+1(G)	1(G)	No	Yes	No
	Fig. 2	2	1(F)+1(G)	1(F)	No	Yes	No
[13]	Figs. 1(a)-(b)	2	2(F)+2(G)	1(G)	No	Yes	Yes
[14]	Fig. 1	1	3(F)+1(G)	1(G)	No	Yes	No
[15]	Fig. 1(a)	1	4(F)+1(G)	1(G)	No	Yes	No
	Fig. 1(c)	1	3(F)+1(G)	1(F)	No	Yes	No
[16]	Fig. 1	1	2(F)+2(G)	1(F)	No	Yes	Yes
[17]	Fig. 1	1	1(F)+1(G)	2(G)	No	Yes	Yes
[18]	Fig. 2(b)	1	1(F)+1(G)	1(F)	No	No	No
[20]	Fig. 2(a)	1	1(F)+1(G)	1(G)	No	No	No
	Fig. 2(b)	1	2(F)+1(G)	1(F)	No	No	No
[23]	Figs. 2-5	1	1(F)+1(G)	1(F)	No	Yes	No
[25]	Fig. 2(b)	1	1(F)+1(G)	1(F)	No	No	No
[26]	Fig. 2(b)	1	2(F)	1(F)	No	Yes	No
	Fig. 2(f)	1	2(F)+1(G)	1(F)	No	No	No
[27]	Fig. 2(c)	1	1(G)	1(G)	No	Yes	No
[28]	Fig. 3	1	2(F)	2(F)	No	Yes	No
[29]	Fig. 13	1	1(G)+1(F)	1(F)	No	Yes	No
[30]	Fig. 3	2	4(F)+1(G)	3(F)	No	No	Yes
Proposed	Fig. 2(a)	1	1(F)	1(G)	Yes	Yes	No

G\* Grounded, F\* Floating

**Table 2** Comparison of proposed parallel R-L simulator with previously reported parallel R-L simulation circuit.

Ref.	Fig. No.	No. of Active Element	No. of Resistors	No. of capacitors	Electronic Control of $L_{eq}$ and $R_{eq}$	Non-Interactive Control of $L_{eq}$	Need for Element Matching
[9]	Fig. 1(a)	1	2(F)	1(F)	No	No	No
[12]	Fig. 2(a)	1	1(F)	1(G)	No	Yes	No
[15]	Fig. 1(b)	1	3(F)+1(G)	1(F)	No	Yes	No
[16]	Fig. 1	1	2(F)+2(G)	1(F)	No	Yes	Yes
[18]	Fig. 2(a)	1	1(F)+1(G)	1(F)	No	Yes	No
[19]	Figs. 2(a)-(b)	2	4(F)	1(F)	No	Yes	No
[20]	Figs. 3(a)-(b)	1	1(F)+1(G)	1(G)	No	No	No
[21]	Figs. 3(a)-(b)	1	1(F)+1(G)	1(F)	No	No	No
[22]	Fig. 2	1	1(F)+1(G)	1(G)	No	No	No
[24]	Fig.1	1	2(F)+2(G)	1(F)	No	No	No
[25]	Fig. 2(c)	1	1(F)+1(G)	1(F)	No	Yes	No
[26]	Fig. 2(c)	1	2(F)+1(G)	1(F)	No	No	Yes
	Fig. 2(d)	1	3(G)	1(F)	No	No	No
	Fig. 2(e)	1	2(F)+1(G)	1(F)	No	Yes	No
[29]	Fig. 4(a)	1	2(G)	1(F)	No	Yes	No
[30]	Fig. 4	2	1(F)+3(G)	3(F)+2(G)	No	Yes	Yes
[31]	Fig. 2(a)	1	2(F)	1(G)	No	No	No
[32]	Fig. 1	1	2(F)	1(F)	No	No	No
	Fig. 2	1	2(F)	1(G)	No	No	No
	Fig. 3	1	3(F)	1(F)	No	No	No
Proposed	Fig. 2(b)	1	1(F)	1(G)	Yes	Yes	No

G\*: Grounded, F\* Floating

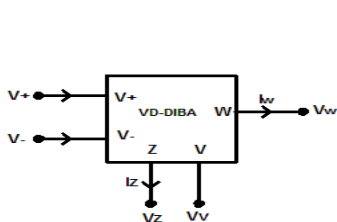


Fig. 1 VD-DIBA Symbol.

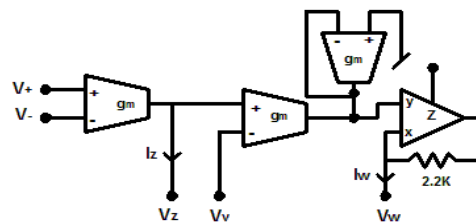


Fig. 2 VD-DIBA Circuit implementation using OTAs and CFOA.

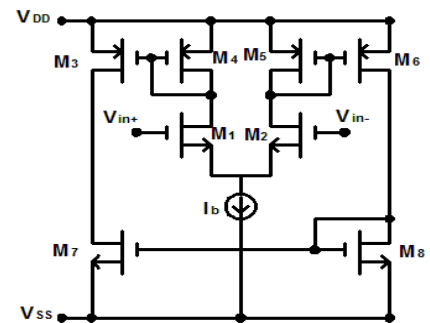


Fig. 3 CMOS realization of OTAs shown in Fig. 2.

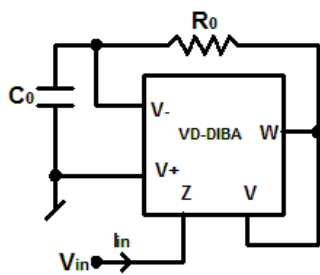


Fig. 4 Presented grounded series R-L simulation circuit.

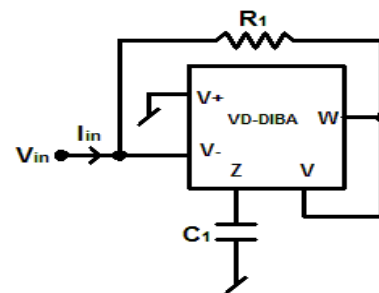


Fig. 5 Presented grounded parallel R-L simulation circuit.

positive types VDDIBAs one grounded capacitance and one floating resistance. Therefore implementation of RLC filters, series/parallel RLC resonance circuits and other useful applications in which grounded series/parallel RL networks are required employing circuit proposed in [34] will require large number of VDDIBAs and resistances as compared to implementation by VDDIBA based lossy inductors proposed in this paper.

### 3 Proposed Configurations

The proposed grounded series R-L and grounded parallel R-L impedance simulation circuits are given in Figs. 4 and 5, respectively. By simple mathematical analysis the expressions of input impedances of configurations shown in Figs. 4 and 5 have been evaluated and given in Table 3.

It can be seen from Table 3, that configurations are shown in Fig. 4 and Fig. 5 are realizing grounded series

**Table 3** Input Impedances of proposed series/parallel RL simulators.

Fig. No.	Input Impedance	Type of Impedance Realized	Equivalent Inductance ( $L_{eq}$ )	Equivalent Resistance ( $R_{eq}$ )
Fig. 4	$\frac{2R_0 s C_0}{g_m} + \frac{2}{g_m}$	$+L_{eq}$ series with $+R_{eq}$	$\frac{2R_0 C_0}{g_m}$	$\frac{2}{g_m}$
Fig. 5	$\frac{1}{\frac{g_m}{2sC_1R_1} + \frac{1}{R_1}}$	$+L_{eq}$ parallel with $+R_{eq}$	$\frac{2C_1R_1}{g_m}$	$R_1$

**Table 4** Input Impedances of proposed series/parallel RL simulators under non-ideal conditions.

Fig. No.	Input Impedance ( $Z_{in}$ )	Type	Equivalent Inductance ( $L_{eq}$ )	Equivalent Resistance ( $R_{eq}$ )
Fig. 4	$\frac{R_0 s C_0}{g_m} \left( \frac{1+\beta^-}{\beta^+} \right) + \frac{1}{g_m} \left( \frac{1+\beta^-}{\beta^+} \right)$	$+L_{eq}$ series with $+R_{eq}$	$\frac{R_0 C_0 (1+\beta^-)}{g_m \beta^+}$	$\frac{1}{g_m} \left( \frac{1+\beta^-}{\beta^+} \right)$
Fig. 5	$\frac{1}{\frac{g_m}{sC_1R_1} \left( \frac{\beta^+}{1+\beta^-} \right) + \frac{1}{R_1}}$	$+L_{eq}$ parallel with $+R_{eq}$	$\frac{R_1 C_1 (1+\beta^-)}{g_m \beta^+}$	$R_1$

R-L and parallel R-L networks. Both the configuration employs single VDDIBA along with single resistance and single capacitance. The placement of grounded capacitor in both circuit configurations makes them suitable for monolithic integration. The series R-L network simulator enjoys the electronic control of both inductive as well as the resistive parts by  $g_m$  along with the independent control of the inductive part by resistance  $R_0$ . Similarly, the parallel R-L simulator has the facility of independent electronic tunability of inductive part by  $g_m$ . To Study the behavior of proposed circuits under different non-ideal circumstances, analysis under non-ideal transfer ratios and analysis under parasitics have been carried out.

#### 4 Non-Ideal Analysis

The voltage-current relationships among between terminals of VDDIBA under non-ideal voltage/transconductance transfer ratios conditions can be defined as;

$$I_Z = \beta_Z g_m (V_{V+} - V_{V-}) \quad (4)$$

$$V_W = \beta^+ V_Z - \beta^- V_V \quad (5)$$

$$I_{V+} = I_{V-} = I_V = 0 \quad (6)$$

where  $\beta^+$  and  $\beta^-$  are the voltage transfer errors and  $\beta_Z$  is transconductance error with a value slightly less than unity. On studying presented VDDIBA based series/parallel R-L simulation circuits under non-ideal conditions, the realized input impedances and their types can be found as given in Table 4.

On comparing the expressions of Table 3 with Table 4, it can be illustrated that the working of proposed simulators with non-ideal constraints remains the same as the ideal behavior. The values of  $R_{eq}$  and  $L_{eq}$  deviate from ideal values but as the values of  $\beta^+$  and  $\beta^-$  are very near to unity, the deviations in values of  $R_{eq}$  and  $L_{eq}$  are very minute. Hence, even taking non-ideal constraints under consideration, the performance of

developed simulators has a closed match with ideal performance.

#### 5 Effects of VDDIBA Terminal Parasitics

In this section, the behavior of proposed series/parallel grounded R-L impedance simulators is evaluated under the presence of parasitic impedances of VDDIBA terminals. At high frequencies, the port parasitics of VDDIBAs become effective and influence the working of VD-DIBA based applications. In CMOS VDDIBA [34] at high frequencies, a finite grounded parasitic resistance  $R_Z$  along with finite grounded parasitic capacitances  $C_Z$  appears at Z ports.

The presented grounded series R-L circuit simulator shown in Fig. 4 is re-evaluated considering the port parasitics of VD-DIBA. The expression of the input impedance is found;

$$Z_{in} = \frac{V_{in}}{I_{in}} = \frac{2R_Z(1+sC_0R_0)}{g_m R_Z + 2(1+sR_Z C_Z)(1+sC_0R_0)} \quad (7)$$

The equivalent circuit configuration developed from (7) has been illustrated in Fig. 6, where

$$L_{eq} = \frac{2R_0 C_0}{g_m} \quad (8)$$

$$R_{eq} = \frac{2}{g_m} \quad (9)$$

Similarly the input impedance of presented parallel R-L simulation circuit given in Fig. 5 under the influence of VD-DIBA port parasitics can be found as;

$$Z_{in} = \frac{V_{in}}{I_{in}} = \frac{R_0(1+sR_Z C_0 + sR_Z C_Z)}{1 + g_m R_Z R_0 + sR_Z(C_0 + C_Z)} \quad (10)$$

The circuit realized from (10) is given in Fig.7, where

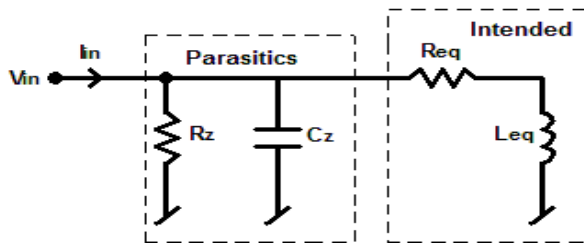


Fig. 6 Proposed Grounded series RL with VDDIBA port parasitic.

$$R_{eq} = R_0 \quad (11)$$

$$R_{eq} = \frac{2(C_1 + C_z)R_1}{g_m} \quad (12)$$

$$R_p = \frac{2R_1}{R_z g_m} \quad (13)$$

So, from Figs. 6 and 7 we can conclude that the influence of VD-DIBA port parasitics on proposed series/parallel R-L simulators is not very adverse.

### 6 Effect of Frequency Dependent Transconductance

The transconductance gain of a VDDIBA is frequency dependent. So, bandwidth limitation of VDDIBA transconductance gain may affect the behavior of proposed circuit at high frequencies. The frequency sensitive transconductance of VDDIBA can be defined by single pole frequency representation as;

$$g_m = \frac{g_{m0}}{1 + s\tau} \quad (14)$$

Here  $\tau = 1/\omega_0$ , where  $\omega_0$  is pole frequency and  $g_{m0}$  is zero frequency transconductance gain.

The input impedance of proposed series R-L circuit simulator considering frequency dependent transconductance is evaluated as;

$$Z_{in} = \frac{2sR_0C_0(1 + s\tau) + 2(1 + s\tau)}{g_{m0}} \quad (15)$$

The impedance  $Z_{in}$  realized by (16) is a grounded network of series resistance  $R_{eq}$ , inductance  $L_{eq}$  and frequency dependent negative conductance (FDNC)  $M_{eq}$ , where

$$L_{eq} = \frac{2(R_0C_0 + \tau)}{g_{m0}} \quad (16)$$

$$R_{eq} = \frac{2}{g_{m0}} \quad (17)$$

$$M_{eq} = \frac{2\tau}{g_{m0}} \quad (18)$$

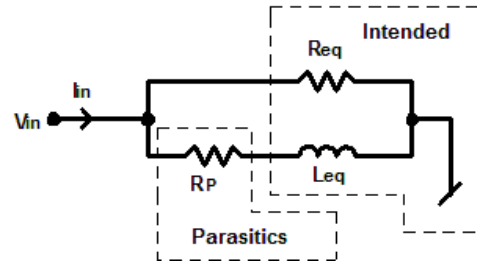


Fig. 7 Equivalent circuit of proposed Grounded Parallel R-L considering parasitics.

So, considering the frequency dependent transconductance, the proposed series R-L configuration behaves like a series  $R_{eq}$ - $L_{eq}$ - $M_{eq}$  circuit where  $M_{eq}$  is the lossy term.

Similarly, the input impedance of proposed parallel R-L circuit simulator considering frequency dependent transconductance is evaluated as;

$$Z_{in} = \frac{2sR_0C_0(1 + s\tau)}{2sR_0C_0(1 + s\tau) + g_{m0}} \quad (19)$$

The impedance  $Z_{in}$  realized by (20) is a passive element network consisting two grounded parallel branches. The first branch consists of a series inductance  $L_{eq}$  along with a frequency dependent negative conductance (FDNC)  $M_{eq}$ . On the other hand the second branch has a resistance  $R_{eq}$ , where

$$L_{eq} = \frac{2R_0C_0}{g_{m0}} \quad (20)$$

$$M_{eq} = \frac{2R_0C_0\tau}{g_{m0}} \quad (21)$$

$$R_{eq} = R_0 \quad (22)$$

So from (21)-(23) it is clear that, considering frequency dependent transconductance, the proposed parallel R-L circuit behaves like a parallel ( $R_{eq}$ )-( $L_{eq}$  series  $M_{eq}$ ) circuit where  $M_{eq}$  is the lossy term.

### 7 Application Examples

The performances of the presented parallel/series R-L simulation circuits are demonstrated by some typical circuit applications. By using proposed series R-L simulation circuit a second order current mode low-pass filtering (LPF) circuit is developed which is shown in Fig. 8.

For demonstrating the working of proposed parallel R-L simulation configuration given in Fig. 5, a voltage-mode high-pass filter (HPF) is constructed and demonstrated in Fig. 9.

### 8 Simulation Results

To validate the mathematical analysis, Simulations were performed under PSPICE environment employing

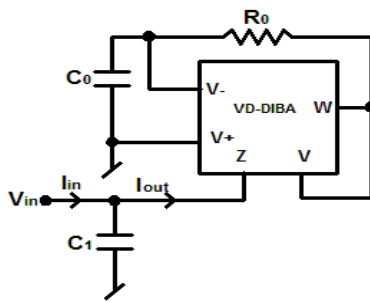


Fig. 8 Current mode LPF developed employing proposed series R-L simulator.

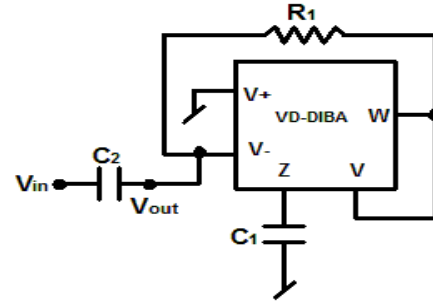


Fig. 9 Voltage mode HPF developed employing proposed parallel R-L simulator.

Table 5 Specification of VDDIBA.

Specification	Value
Input voltage linear range	-120 to 120 [mV]
3 dB bandwidth	121 [MHz]
Power consumption	62.5 [mW]
Transconductance gain	258.091 [ $\mu$ A/V]

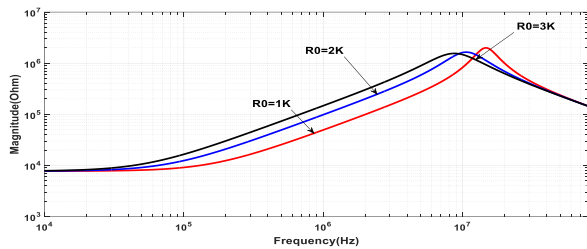


Fig. 10 Frequency responses of impedance of proposed series R-L simulator.

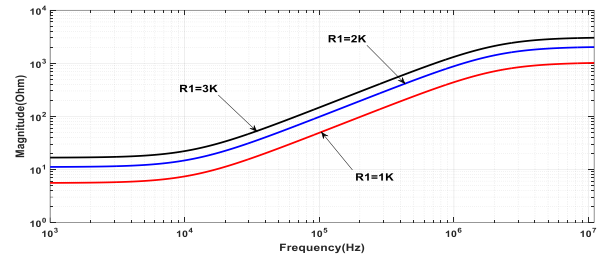


Fig. 11 Frequency responses of impedance of presented parallel R-L simulation circuit.

CMOS VDDIBA which includes CMOS OTA and CFOA SPICE micro-model of AD844. The DC supply voltages were chosen as  $\pm 0.9$  VDC with all the biasing current of VDDIBA equals to  $32 \mu\text{A}$ . The main specifications of this VDDIBA are given in Table 5.

Series R-L simulator of Fig. 2 is simulated with  $R_0 = 1, 2$  and  $3\text{k}\Omega$  and  $C_0 = 1\text{nF}$ . The magnitude responses of the input impedance of configuration described in Fig. 4 have been illustrated in Fig. 10. From input impedance expression of Fig. 4 given in Table 3, it is observed that at low frequencies the inductive part of realized impedance  $L_{eq}$  is very small in comparison to the lossy term  $R_{eq}$ . Therefore, the magnitude responses are almost constant for low frequencies and representing the  $R_{eq}$ . As the frequency increases, the value of  $L_{eq}$  start increasing in comparison to constant lossy part  $R_{eq}$  and the circuit start behaving like a series lossy inductor. At very high frequencies, the value of  $L_{eq}$  becomes very high in comparison to  $R_{eq}$  and the configuration acts as a pure lossless inductor. This effect can be illustrated by plots shown in Fig. 8 The initial “horizontal part” of frequency response is due to the dominance of lossy term  $R_{eq}$ . Similarly the PSPICE simulated responses of impedance of parallel R-L network described in Fig. 5 have been illustrated in Fig. 10, for component values  $R_0 = 1, 2$  and  $3\text{k}\Omega$ , and  $C_0 = 0.01\text{nF}$ .

From input impedance expression of Fig. 4 given in Table 3, it can be seen that for the high value of  $C_0$ , the value of  $L_{eq}$  is high in comparison to lossy part  $R_{eq}$  and behavior of this series lossy inductor become inclined more towards a lossless inductor. For further high values of  $C_0$ , the value of  $R_{eq}$  will be very small in comparison to  $L_{eq}$  and the configuration will work as a pure lossless inductor. This effect can be illustrated by response plots shown in Fig. 12. The initial “horizontal part” of frequency response is due to the existence of the lossy term  $R_{eq}$ . As the value of  $C_0$  increases, the value of  $L_{eq}$  becomes high and flat part of response become comparatively narrower than inclined part. Which clearly indicate that on increasing  $C_0$  the behavior of the proposed circuit starts inclining towards the behavior of a lossless inductor. Similarly the magnitude plots of impedance of parallel R-L network given in Fig. 5 on varying capacitance  $C_1$  have been given in Fig. 13.

To demonstrate the electronic controllability of developed series R-L simulator shown in Fig. 4, simulations were performed with different bias current values. With component values  $R_0 = 1\text{k}\Omega$  and  $C_0 = 1\text{nF}$ , bias currents were selected as  $I_b = 32, 48,$  and  $64 \mu\text{A}$ . The simulation plots are shown in Fig. 14 which clearly illustrates that on increasing the bias currents,  $g_m$  is increasing and the input impedance is decreasing.

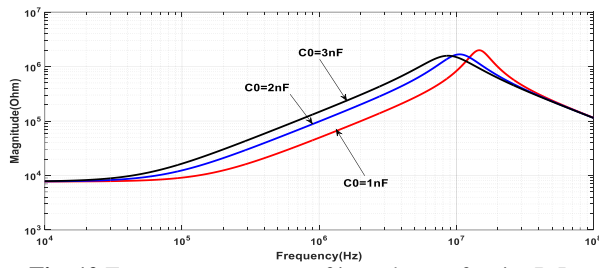


Fig. 12 Frequency responses of impedance of series R-L simulator with different values of  $C_0$ .

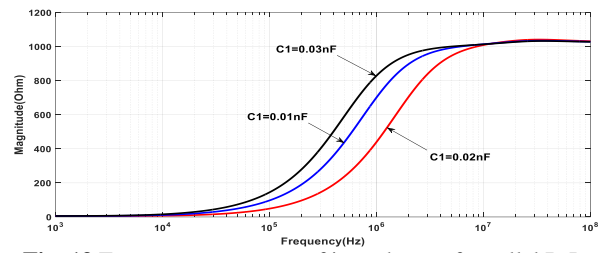


Fig. 13 Frequency responses of impedance of parallel R-L simulator with diverse values of  $C_1$ .

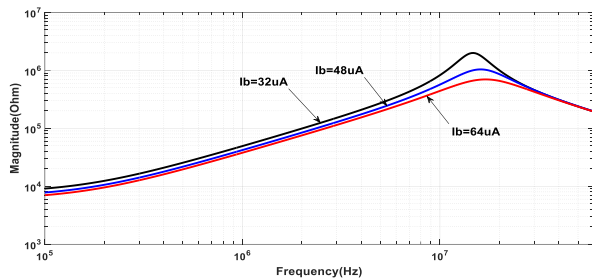


Fig. 14 Frequency responses of impedance of series R-L simulator for different values of biasing currents.

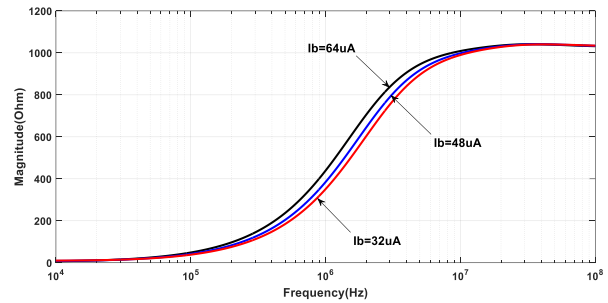


Fig. 15 Frequency responses of parallel R-L simulation circuit for different values of biasing currents.

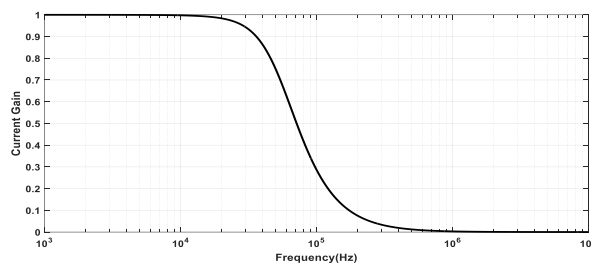


Fig. 16 The frequency response from current-mode low-pass filtering circuit given in Fig. 8.

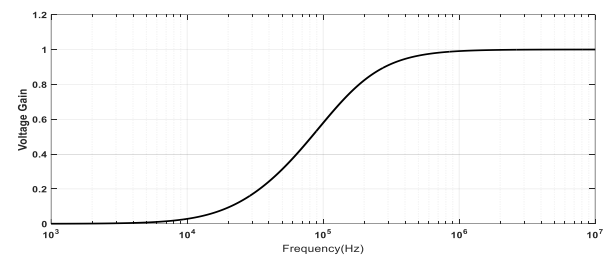


Fig. 17 The frequency response of voltage-mode high-pass filtering circuit given in Fig. 9.

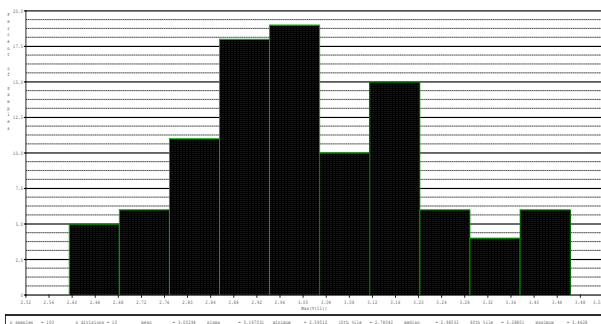


Fig. 18 Monte-Carlo simulation results of circuit shown in Fig. 8.

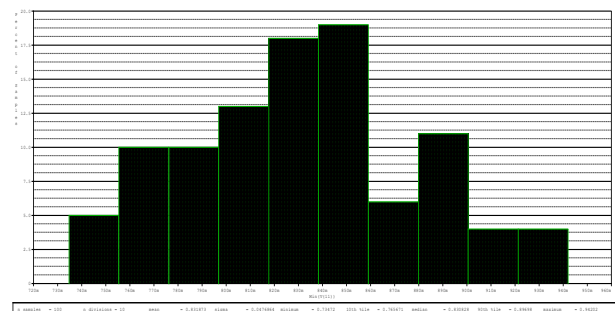


Fig. 19 Monte-Carlo simulation results of circuit shown in Fig. 9.

Electronic tunability of parallel R-L simulator shown in Fig. 5 has been demonstrated in plots shown in Fig. 15 with component values  $R_1 = 1 \text{ k}\Omega$  and  $C_1 = 0.01 \text{ nF}$ . The current mode LPF design example shown in Fig. 8 is simulated with passive component values selected as  $C_0 = 0.01 \text{ nF}$ , and  $C_1 = 0.02 \text{ nF}$ . The simulated filter response is shown in Fig. 16. For simulation of HPF shown in Fig. 9, following component values are chosen:  $C_1 = 0.02 \text{ nF}$ , and  $C_2 = 0.01 \text{ nF}$ . The frequency

response of this HPF is given in Fig. 17. To verify the robustness, the Monte-Carlo simulations of developed filtering circuits shown in Figs. 8 and 9 have been performed on taking 100 samples and 5% variation in passive element values. The Monte-Carlo simulation results are demonstrated in Figs. 18 and 19 respectively.

## 9 Conclusion

This paper proposes a new grounded series/parallel



R-L Network simulators using VDDIBA. In literature, several grounded series/parallel R-L network simulation circuits employing various active elements have been reported. These reported circuits suffer from one or more of following disadvantages; Use of more than one active element [11, 19, 30], employment of more than one resistance [10-11, 13-32], requirement of floating capacitance [9-11, 15-16, 18-21, 23-26, 28-30, 32], unavailability of electronic tuning facility of both inductive as well as resistive part [9-32], lack of independent control of realized inductance [11, 18, 20, 25, 26, 30] and need of matched elements [9, 20-24, 26, 31, 32]. The series R-L and parallel R-L simulation circuits presented in this paper are very compact with minimum requirement of passive and active components (one VDDIBA, single capacitance and single resistance) and enjoy several advantageous characteristics like use of grounded capacitor, facility of electronic tuning, non-interactive tuning of equivalent inductance and no need of any element value matching. Under non-ideal conditions, the behavior of presented circuits was found un-deviated from their ideal behavior. The influence of port parasitics of VDDIBA and effect of frequency dependent transconductance was also studied. To check the workability of presented circuits, some application examples are given. PSPICE simulations with 0.18  $\mu\text{m}$  TSMC CMOS model were included to confirm the theoretical results

## References

- [1] A. J. Prescott, "Loss compensated active gyrator using differential input operational amplifier," *Electronics Letters*, Vol. 2, No. 7, pp. 283–284, 1966.
- [2] R. Senani, "Active simulation of inductors using current conveyors," *Electronics Letters*, Vol. 14, No. 15, pp. 483–484, 1978.
- [3] R. Senani, "New Tunable synthetic floating inductors," *Electronics Letters*, Vol. 6, No. 10, pp. 382–383, 1978.
- [4] A. E. Cam. and O. Cicekoglu "Novel lossless grounded inductance simulators employing only a single first generation current conveyor," *Frequenz; Journal of RF Engineering and Telecommunication*, Vol. 57, pp. 204–206, 2003.
- [5] E. Yuce, "Grounded inductor simulators with improved low frequency performances" *IEEE Transactions on Instrumentation and Measurement*, Vol. 57, No. 5, pp. 1079–1084, 2008.
- [6] D. Prasad, D. R. Bhaskar, and A. K. Singh "New grounded and floating simulated inductance circuits using current differencing transconductance amplifiers," *Radioengineering*, Vol. 19, No.1, pp. 194–198, 2010.
- [7] F. Kacar, "New lossless inductance simulators realization using a minimum active and passive components," *Microelectronics Journal*, Vol. 41, No. 2–3, pp. 109–113, 2010.
- [8] D. Prasad and D. R. Bhaskar, "Grounded and floating inductance simulation circuits using VDTAs," *Circuits and Systems*, Vol. 3, No. 4, pp. 342–347, 2012.
- [9] R. L. Ford and F. E. G. Girling "Active filters and oscillators using simulated inductance," *Electronics Letters*, Vol. 2, No. 2, pp. 481–482, 1966.
- [10] R. Nandi, "Inductor Simulation Using a Current Conveyor," *Proceedings of the IEEE*, Vol. 65, No. 10, pp. 1511–1512, 1977.
- [11] R. Nandi "Active inductances using current conveyors and their application in a simple bandpass filter realization," *Electronics Letters*, Vol. 14, No. 12, pp. 373–374, 1978.
- [12] A. M. Soliman, "Grounded inductance simulation using the DVCCS/DVCVS," *Proceedings of the IEEE*, Vol. 66, No. 9, pp. 334–336, 1979.
- [13] R. Nandi, "Insensitive grounded-capacitor simulation of grounded inductors using current conveyors" *Electronics Letters*, Vol. 15, No. 21, pp. 693–696, 1979.
- [14] R. Senani and R. N. Tiwari, "New canonic active RC realizations of grounded and floating inductors," *Proceedings of the IEEE*, Vol. 66, No. 7, pp. 803–804, 1978.
- [15] R. Senani :Reply by R. Senani to "Comment on "New canonic active RC Realizations of grounded and floating inductors"",". *Proceedings of the IEEE*, Vol. 70, No. 1, pp. 803–804 1982.
- [16] A. N. Paul and D. Patranabis, "Active simulation of grounded inductors using a single current conveyor," *IEEE Transactions on Circuits and Systems*, Vol. 28, No. 2, pp. 164–165, 1981.
- [17] S. J. Liu and Y.S. Hwang, "Realisation of R-L and C-D impedances using a current feedback amplifier and its applications," *Electronics Letters*, Vol. 3, No. 5, pp. 380–381, 1994.
- [18] H. Y. Wang and C. T. Lee, "Realisation of R-L and C-D immittances using single FTFN," *Electronics Letters*, Vol. 34, No. 6, pp. 502–503, 1998.
- [19] U. Cam, O. Cicekoglu, H. Kuntman, and A. Kuntman "Novel two OTRA-based grounded immittance simulator topology," *Analog Integrated Circuits and Signal Processing*, Vol. 39, No. 2, pp. 169–175, 2004.



- [20] M. Incekaraoglu and U. Cam, "Realization of series and parallel R-L and C-D impedances using single differential voltage current conveyor," *Analog Integrated Circuits and Signal Processing*, Vol. 43, No. 3, pp. 101–104, 2006.
- [21] E. Yuce, S. Minaei, and O. Cicekoglul, "Limitations of the simulated inductors based on a single current conveyor," *IEEE Transactions on Circuits and Systems*, Vol. 53, No. 12, pp. 2860–2867, 2006.
- [22] E. Yuce, "Comment on "realization of series and parallel R-L and C-D impedances using single differential voltage current conveyor","" *Analog Integrated Circuits and Signal Processing*, Vol. 49, No. 1, pp. 91–92, 2006.
- [23] E. Yuce, "Novel lossless and lossy grounded inductor simulators consisting of a canonical number of components," *Analog Integrated Circuits and Signal Processing*, Vol. 59, No. 1, pp. 77–82, 2009.
- [24] P. Kumar and R. Senani "New grounded simulated inductance circuit using a single PFTFN. *Analog Integrated Circuits and Signal Processing*, Vol. 62, No. 1, pp. 105–112, 2010.
- [25] F. Kacar and H. Kuntman "CFOA-based lossless and lossy inductance simulators," *Radioengineering*, Vol. 20, No. 3, pp. 627–631, 2011.
- [26] B. Metin "Supplementary inductance simulator topologies employing single DXCCII," *Radioengineering*, Vol. 20, No. 3, pp. 614–618, 2011.
- [27] F. Kacar, A. Yesil, S. Minaei, and H. Kuntman "Positive/negative lossy/lossless grounded inductance simulators employing single VDCC and only two passive elements.," *International Journal of Electronics and Communication (AEU)*, Vol. 68, No. 1, pp. 73–78, 2014.
- [28] A. Gupta, R. Senani, D.R. Bhaskar and A. K. Singh "OTRA-based grounded-FDNR and grounded-inductance simulators and their applications," *Circuits Syst Signal Process*, Vol. 31, No. 2, pp. 489–499, 2012.
- [29] M. Higashimura and Y. Fukuji "Realization of immittance function using a single FTFN and its application to filter," in *IEEE International Symposium on Circuits and Systems*, Vol. 2, pp. 41–46, 1992.
- [30] U. Cam, O. Cicekoglul and H. Kuntman "Universal series and parallel immittance simulators using four terminal floating nullors, *Analog Integrated Circuits and Signal Processing*, Vol. 25, pp. 59–66, 2000.
- [31] J. K. Pathak, A. K. Singh, and R. Senani, "New canonic lossy inductor using a single CDDBA and its application," *International Journal of Electronics*, Vol. 103, No. 1, pp. 1–13, 2016.
- [32] M. Gulsoy, "Lossless and lossy synthetic inductors employing single current differencing buffered amplifier," *IEICE Transactions on Communications*, Vol. 88, No. 5, pp. 2152–2155, 2005.
- [33] D. Bielek, R. Senani, V. Biolkova, and Z. Kolka "Active elements for analog signal processing; classification, review and new proposals," *Radioengineering*. Vol. 17, No. 4, pp. 15–32, 2008.
- [34] D. Prasad, D. R. Bhaskar, and K. L. Pushkar, "Realization of new electronically controllable grounded and floating simulated inductance circuits using voltage differencing differential input buffered amplifiers," *Active and Passive Electronic Components*, Vol. 2011, pp. 8, 2011.
- [35] D. R. Bhaskar, K. L. Pushkar And D. Prasad "Electronically-controllable grounded-capacitor-based grounded and floating inductance simulated circuits using VD-DIBAs," *Circuits and Systems*, Vol. 4, No. 5, pp. 422–430, 2011.
- [36] D. Bielek and V. Biolkova "First-Order voltage-mode all-pass filter employing one active element and one grounded capacitor," *Analog Integrated Circuits and Signal Processing*, Vol. 65, No. 1, pp. 123–129, 2010.
- [37] W. Jiakala, D. Bielek, S. Siripongdee, and J. Bejar, "High input impedance voltage-mode biquad filter using VD-DIBA's," *Radioengineering* , Vol. 23, No. 3, pp. 914–921, 2014.

**M. Srivastava** obtained Ph.D. in analog integrated circuits and signal processing from Jamia Millia Islamia, New Delhi, India, in 2015. Presently he is working as a Assistant Professor with Department of Electronics and Communication Engineering, National Institute of Technology, Jamshedpur, India. His research interest is in the areas of analog circuits. Dr. Srivastava has authored or co-authored 42 research papers in SCI/Scopus indexed International Journals and Conferences. He acted as reviewer of various SCI Indexed international journals and worked as a member of Technical Program Committee/ Reviewer/ Session Chair in several international conferences in India and abroad.

**K. Bhardwaj** was born in Hathras India in 1998. In 2016 he competed Diploma in Electronics Engineering from Government Polytechnic College, Hathras. Currently he is a B. Tech. student and research scholar with Dr. A. P. J. Abdul Kalam University, Lucknow, India. Kapil's research interest includes analog circuits and analog signal processing. He has authored several papers in reputed conference proceedings.



© 2019 by the authors. Licensee IUST, Tehran, Iran. This article is an open access article distributed under the terms and conditions of the Creative Commons Attribution-NonCommercial 4.0 International (CC BY-NC 4.0) license (<https://creativecommons.org/licenses/by-nc/4.0/>).